Development of a simplified method for the assessment of liquefaction mitigation via vertical gravel drains

Gabriele Boccieri [i)], Domenico Gaudio [ii)], Riccardo Ronci [iii)] and Riccardo Conti [iv)]

i) Ph.D Student, Engineering Department, Università di Roma Niccolò Cusano, Via Don Carlo Gnocchi 3, 00166, Rome, Italy.
ii) Assistant Professor, Department of Structural and Geotechnical Engineering, Sapienza Università di Roma, Via Eudossiana 18, 00184, Rome, Italy.
iii) Ph.D Student, Department of Civil Engineering and Computer Science Engineering, Università degli Studi di Roma Tor Vergata, Via del Politecnico 1, 00133, Rome, Italy.
iv) Associate Professor, Department of Civil Engineering and Computer Science Engineering, Università degli Studi di Roma Tor Vergata, Via del Politecnico 1, 00133, Rome, Italy.

ABSTRACT

Seismic–induced liquefaction of saturated sandy soils may cause severe damage to civil infrastructures, pushing the scientific community toward a more in-depth understanding of the physical phenomenon and the development of effective strategies for its mitigation. Vertical gravel drains and stone columns are often used as a mitigation measure against liquefaction as, depending on site conditions, they can be easier to install and more cost-effective with respect to other design solutions. Standard design methods of the gravel drains are usually based on the seminal work by Seed and Booker (1977), which relies on several simplifying assumptions about: the direction of water flow (purely horizontal axisymmetric flow towards the drains), the physical and mechanical properties of the drain material (virtually infinite permeability), and the rate of excess pore pressure (described through empirical relationships based on undrained cyclic tests).
The present paper illustrates a comparison between the seminal work proposed by Seed and Booker, which was subsequently improved by Onoue (1988), and the results of a fully-coupled, nonlinear dynamic 3D Finite Element analysis, where the cyclic behaviour of the saturated sand layer is described through an advanced constitutive model.

Keywords: liquefaction, gravel drains, simplified method, Finite Element Analysis

1 INTRODUCTION

Liquefaction phenomena, induced in saturated sandy soils by medium-to-high intensity earthquakes, may lead to dramatic consequences for civil infrastructures. The fully or partially undrained behaviour exhibited by sandy layers results in the development of excess pore water pressures, which reduce the effective stress state into the soil and, consequently, its shear stiffness and strength.

The risk of liquefaction and associated ground deformations can be reduced by various ground-improvement methods, including gravel drains, densification, and cementation. Use of gravel drains is probably the most common method for mitigating earthquake-induced liquefaction, because the construction method is relatively simple and cost-effective.

Design methods for gravel drains are mainly based on the seminal work by Seed and Booker (1977), which relies on several simplifying assumptions: (i) purely horizontal axisymmetric water flow towards the drain; (ii) infinitely permeable drain; and (iii) adopting empirical relations, based on undrained cyclic laboratory tests, to compute the seismic-induced excess pore water pressures (Seed *et al.*, 1975).

Although many experimental and numerical works have been published so far, aiming at extending the work by Seed and Booker to more realistic conditions (Onoue, 1988; Bouckovalas *et al.*, 2011), or at providing further insight into the effectiveness of vertical drains in reducing excessive pore-pressures build-up (Elgamal *et al.*, 2009), stone column design techniques are still based on heuristic rules and procedures developed through practical experience.

This paper aims to study the reliability of the original work proposed by Seed and Booker, and subsequently improved by Onoue (1988). To this end, the simplified method is implemented in a home-made *Matlab* routine through the Finite Difference Method (FDM), and compared against the results of coupled dynamic Finite Element (FE) analyses, where sand behaviour is described through the advanced constitutive model proposed by Dafalias and Manzari (2004).

An axisymmetric configuration was considered, characterised by three 1-m-thick soil strata, with a liquefiable sand lying between two clayey layers, and a

gravel drain with radius $r_d = 0.5$ m (Fig. 1). The water table is located at the ground surface and the initial pore pressure regime is hydrostatic.

2 SIMPLIFIED METHOD

Seed *et al.* (1975) proposed a simplified approach to evaluate the generation and redistribution of seismic-induced excess pore water pressures, u, in a stratified soil deposit, in the absence of gravel drains. The Authors modified the well-known 1D consolidation equation (Terzaghi, 1923), by adding a source term due to earthquake shaking (Boccieri *et al.*, 2022). Seed and Booker (1977) extended the work by Seed *et al.* (1975) to the case of axisymmetric conditions in the presence of a drain, considering vertical and radial water flow:

$$\frac{\partial u(r,z,t)}{\partial t} = c_{vh} \cdot \left(\frac{\partial^2 u}{\partial r^2} + \frac{1}{r} \cdot \frac{\partial u}{\partial r} \right) + c_{vz} \cdot \frac{\partial^2 u}{\partial z^2} + \frac{\partial u_g}{\partial t} \quad (1)$$

where r is the distance from the center of the drain and z the depth (Fig. 1). The first and second terms on the right-hand side of Eq. (1) are dissipative terms, in cylindrical coordinates, proportional to the horizontal and vertical consolidation coefficient, c_{vh} and c_{vz}, while the third one is a source term, representing the rate of excess pore water pressures occurring in fully undrained conditions.

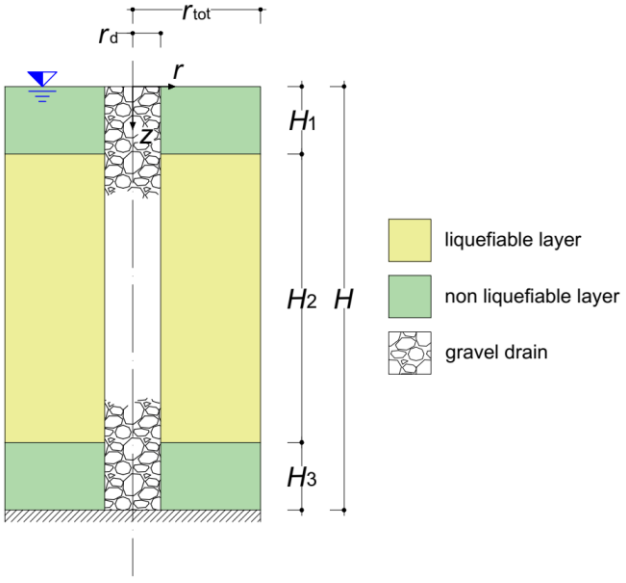

Fig. 1. Problem layout in its axisymmetric configuration.

As for the dissipative terms, the degradation of the consolidation coefficients, due to the seismic-induced excess pore water pressures, was considered in this work using a standard equation for sands:

$$c_v = \frac{k \cdot E_{oed}}{\gamma_w} \quad (2a)$$

$$E_{oed} = \frac{2 \cdot G_0 \cdot (1-\nu)}{(1-2\cdot\nu)} \quad (2b)$$

$$G_0 = F(e) \cdot (p')^{0.5} \quad (2c)$$

where k, E_{oed} and ν are the soil hydraulic conductivity, oedometric modulus and Poisson's ratio, respectively; γ_w is the unit weight of water; G_0 is the small-strain shear stiffness; $F(e)$ is a function of the void radio e; and p' is the mean effective stress, the latter depending on the excess pore water pressure, u.

The generative term $\partial u_g/\partial t$, as in Seed *et al.* (1975), is related to the seismic-induced shear stress $\tau(t)$ through an equivalent cyclic load, which is characterized by a constant amplitude, $\tau_{eq} = 0.65 \cdot \tau_{max}$, and by a number of cycles N_{eq}, uniformly distributed over the cyclic loading duration T_d. Hence, the source term can be written as:

$$\frac{\partial u_g}{\partial t} = \frac{\partial u_g}{\partial N} \cdot \frac{\partial N}{\partial t} = \frac{\sigma'_{v0}}{N_L} \cdot \frac{\partial r_u}{\partial r_N} \cdot \frac{N_{eq}}{T_d} \quad (3)$$

where $r_u = u_g/\sigma'_{v0}$ is the excess pore pressure ratio; $r_N = N/N_L$ is the cyclic ratio; N is the n^{th} cycle of loading, and N_L is the number of cycles to trigger liquefaction ($u_g = \sigma'_{v0}$). If the correlation between r_u and r_N is known, together with N_L, N_{eq} and T_d, then the rate of excess pore water pressures under fully undrained conditions, $\partial u_g/\partial t$, can be computed via Eq. (3).

Seed and Booker (1977) introduced two simplifying assumptions to solve Eq. (1):

i) Infinitely permeable drain, which corresponds to assuming zero pore pressure at the drain-soil interface;

ii) purely horizontal water flow toward the drain, thus reducing the study to an axial-symmetric configuration where the sole radial coordinate is considered ($\partial^2 u/\partial r^2 \neq 0$; $\partial u/\partial r \neq 0$ and $\partial^2 u/\partial z^2 = 0$ in Eq.(1)).

Onoue (1988) removed these two hypotheses and solved Eq. (1) considering a flow continuity condition at the interface between the drain and the liquefiable soil and both horizontal and vertical flow into the soil domain ($\partial^2 u/\partial r^2 \neq 0$; $\partial u/\partial r \neq 0$ and $\partial^2 u/\partial z^2 \neq 0$ in Eq.(1)). The flow continuity condition at the drain-soil interface is:

$$\frac{k_d}{k_s} \cdot \frac{r_d}{2} \cdot \left. \frac{\partial^2 u}{\partial z^2} \right|_{r=r_d} + \left. \frac{\partial u}{\partial r} \right|_{r=r_d} = 0 \quad (4)$$

where k_d and k_s are the vertical hydraulic conductivity of the drain and the horizontal hydraulic conductivity of the soil, respectively.

The simplified method introduced by Seed and Booker (1977), and later improved by Onoue (1988), was implemented in *Matlab v.9.10.0 (R2021a)* (Mathworks Inc., 2021) through the Finite Difference Method (FDM), considering:

i) initial excess pore water pressures equal to zero ($u(t=0) = u_0 = 0$);

ii) null excess pore water pressures at the groundwater level;

iii) impervious boundary conditions at the

bottom of the domain ($z = H$) and at the maximum distance from the drain r_{tot}, equal to half the centre-to-centre distance between two adjacent drains:

$$\left.\frac{\partial u}{\partial z}\right|_{z=H} = 0 \tag{5a}$$

$$\left.\frac{\partial u}{\partial r}\right|_{r=r_{tot}} = 0 \tag{5b}$$

iv) flow continuity at the interface between the drain and the liquefiable soil (Eq.(4)).

The assumptions introduced for the curve r_u-r_N, together with the evaluation of N_L, N_{eq}, and T_d, are discussed in the following.

2.1 Excess pore water pressures relationship and cyclic resistance curve

Seed and Booker (1977) expressed r_u as a function of r_N after fitting the results of undrained cyclic laboratory tests:

$$r_u = \frac{2}{\pi} \cdot \sin^{-1}\left(r_N^{1/2\alpha}\right) \tag{6}$$

with $\alpha = 0.7$. This relation has been retained in this work.

The number of cycles needed to trigger liquefaction, N_L, is typically obtained from experimental cyclic resistance curve CSR-N_L, with the following form:

$$CSR = \beta \cdot N_L^{-\eta} \tag{7}$$

where the cyclic stress ratio $CSR = 0.65 \cdot \tau_{max}/\sigma'_{v0}$ can be derived either from simplified procedures or proper seismic response analyses. In this work, a simplified procedure is used to estimate CSR based on the equilibrium of a soil column subject to a uniform horizontal acceleration (Seed and Idriss, 1971):

$$CSR = \frac{\sigma_{v0}(z)}{\sigma'_{v0}(z)} \cdot \frac{0.65 \cdot a_{max}}{g} \cdot (1 - 0.015 \cdot z) \tag{8}$$

where z is the depth (in meters); σ_{v0} and σ'_{v0} are the total and effective vertical geostatic stresses, respectively; a_{max} is the maximum acceleration of the input motion, and g is the gravitational acceleration.

2.2 Equivalent cyclic loading and its duration

The irregular shear stress time history induced by the seismic event is replaced by an equivalent cyclic loading, with a constant amplitude τ_{eq} and a number of equivalent cycles N_{eq} distributed uniformly over the duration T_d.

The evaluation of N_{eq} is based on the hypothesis of the linear damage accumulation proposed by Miner (1945), considering the CSR-N_L curve as the *locus* of same damage level (*i.e.* triggering of soil liquefaction). Following this assumption, N_{eq} can be computed as:

$$N_{eq} = \sum_i N_i \cdot \left(\frac{CSR_{eq}}{CSR_i}\right)^{-1/\eta} \tag{9}$$

where N_i is the number of cycles with amplitude CSR_i and $CSR_{eq} = 0.65 \cdot \tau_{max}/\sigma'_{v0}$. The term CSR_i was computed through Eq. (8), by simply replacing $0.65 \cdot a_{max}$ with a_i.

A method for calculating the number of cycles of the irregular signal was therefore necessary. To this end, the peak-counting method was adopted, where the largest peaks between adjacent zero-crossing are only counted (Hancock and Bommer, 2005). In this way, every peak considered identifies a hemicycle, and $N_i = 0.5$ in Eq. (9).

The duration of the cyclic loading, T_d, was assumed equal to the strong motion duration of the input acceleration time history, which is defined as the time interval between the time instants when the Arias intensity, I_A, reaches 5% and 95% of its maximum (Trifunac and Brady, 1975).

3 COMPARISON WITH COUPLED FE ANALYSIS

The simplified method implemented in *Matlab* was compared against the results of a 3D dynamic coupled FE analysis, performed with the code *Plaxis 3D* v21.01 (Bentley Systems, 2021).

3.1 3D coupled FE dynamic analysis

The numerical model is shown in Fig. 2. The soil deposit is characterized by three 1-m-thick horizontal soil layers, with the top and the bottom ones consisting of clay, while the middle one is liquefiable sand, as in the reference layout. A triangular grid composed of three gravel drains is considered, with a radius of 0.5 m and a centre-to-centre distance of 2.5 m. The water table is at the ground level.

The mesh consists of 10-noded tetrahedral elements with a height of 0.25 m, except for the 6-m-wide central portions of the upper and lower layers, where the height is halved (0.125 m). The mesh is composed by 17382 elements and 27319 nodes.

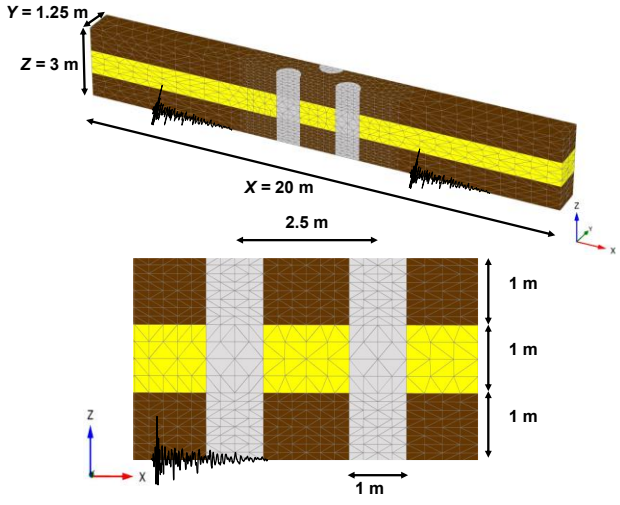

Fig. 2. 3D FE model implemented in *Plaxis 3D v21*.

Fig. 3 shows (a) the acceleration time history and (b) the Fourier Amplitude spectrum of the applied input motion, recorded during the Hollister (1961) earthquake. The signal was preliminary low-pass filtered at 10 Hz and then applied at the model base along the *x*-direction. Relevant ground motion parameters of the input motion are also given in Fig. 3, where f_p is the predominant frequency (Kramer, 1996).

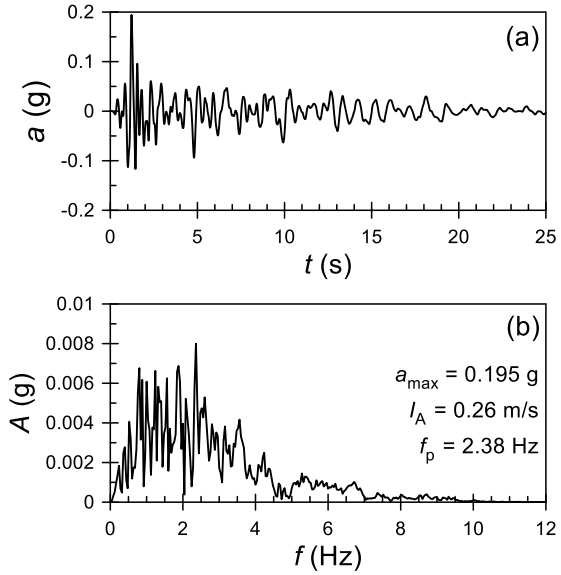

Fig. 3. Acceleration time history (a) and Fourier Amplitude Spectra (b) of the Hollister (1961) earthquake.

The analysis was carried out in three steps:

i) geostatic phase (k_0 *procedure*), to compute the lithostatic effective stress state in the soil domain, without any drain;
ii) activation of the drains;
iii) fully-coupled dynamic phase, in which the input motion is applied at the bottom. This stage is solved using the classical *u-p* formulation (Zienkiewicz *et al.*, 1980).

The nodes on the lateral *x-z* boundaries were normally fixed in all the calculation steps, while the bottom boundary (*x-y* plane) was fully fixed during the static phase and assigned the input motion along the *x* direction in the dynamic one. The nodes along the vertical *y-z* boundaries were normally fixed during the first two steps and assigned a *free-field* condition in the third one. As for the hydraulic boundary conditions, all surfaces were impervious, except for the ground water table, where a zero pore pressure was imposed (*i.e.*, drained boundary).

Table 1 shows the main physical properties of the soil materials. In the FE analysis, the mechanical behaviour of the clay was described through the *Hardening Soil with Small Strain Stiffness* constitutive model (Benz *et al.*, 2009), while the sandy layer and the gravel drains were assigned the SANISAND04 model (Dafalias and Manzari, 2004). As for the values adopted for the model parameters, those from Gaudio and Rampello (2019) were adopted for the clay layers, whereas both the sand and gravel materials were assigned the values representative of the Toyoura sand, retrieved from Dafalias and Manzari (2004). In order to prevent volumetric-deviatoric coupling for the gravel material, thus inhibiting any pore water pressure build-up within the gravel drains, the constitutive parameter $A_0 = 0.01$ was adopted in the SANISAND04 model.

Table 1. Soil properties adopted in the numerical model.

soil	G_s (-)	e_0 (-)	D_R (%)	*OCR* (-)	k (m/s)
clay	2.75	-	-	2.0	1e-7
sand	2.75	0.825	40	-	1e-4
gravel	2.75	0.825	40	-	1e-2

G_s = specific gravity; e_0 = initial void ratio; D_R = relative density; *OCR* = overconsolidation ratio; k = hydraulic conductivity.

3.2 Calibration of the simplified method

In order to calibrate the two coefficients defining the cyclic resistance curve *CSR*-N_L in Eq. (7), a series of Cyclic Undrained Shear Tests (CUST in the following) on a liquefiable sand element was simulated by Mazzola and Lombardi (2021) with the *Soil Test* tool available in *Plaxis*. In all tests, the following parameters were adopted: $\sigma'_{v0} = 150$ kPa, $k_0 = 0.5$, and $f = 1$ Hz (frequency of the sinusoidal shear stress time history applied atop the soil element). The simulated tests differ each other as for the applied *CSR*, which varies between 0.05 and 0.4. Fig. 4 shows the results of the best-fitting procedure, together with the relevant coefficients β and η. Taking the middle depth of the liquefiable layer as reference ($z = 1.50$ m in Eq. (8)), the number of cycles to liquefaction and the equivalent one were computed accordingly, obtaining $N_L = 1.58$ and $N_{eq} = 6.68$.

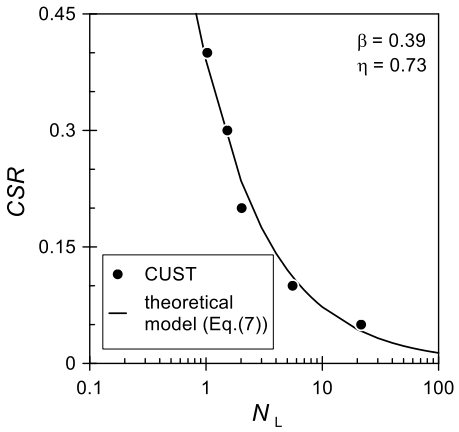

Fig. 4. Cyclic resistance curve adopted in the simplified method.

3.3 Comparison of results

Fig. 5 compares the time histories of the excess pore water pressure ratio r_u computed via the coupled FE analysis and the simplified method at three depths within the liquefiable sandy layer ($z = 1$ m, 1.5 m and 2 m).

At all depths, the excess pore pressure ratio r_u from coupled analysis shows a rapid increase during the early

stage of the event, reaching a peak value $r_{u,\,max} \approx 0.8$, followed by dissipation right after about 5 s, indicating a proper functioning of the drains. The time histories of r_u predicted by the simplified method differ significantly from the numerical ones, both in the generative and in the dissipative phase. Indeed, the results of the simplified method show triggering of liquefaction ($r_u = 1$) in the sand layer right after 7 s, keeping constant up to about 17 s, when a rapid dissipation process takes place.

These large discrepancies may be attributed to the following assumptions underlying the simplified method by Seed and Booker (1977):

i) The number of equivalent cycles N_{eq} should be actually computed from a Site Response Analysis (SRA), which would result in a variation with depth rather than in a constant value;

ii) Considering a uniform distribution of the equivalent cycles over the loading duration ($\partial N/\partial t = N_{eq}/T_d$ in Eq. (3)) does not represent adequately the evolution in time of the energy content of the earthquake loading. This results in a unrealistic balance between the generative and dissipative processes during the seismic event;

iii) Neglecting the stiffness degradation and filtering of the signal propagating within the liquefiable sand, both due to pore pressure build-up, may lead to a gross overestimation of the equivalent number of cycles, N_{eq}.

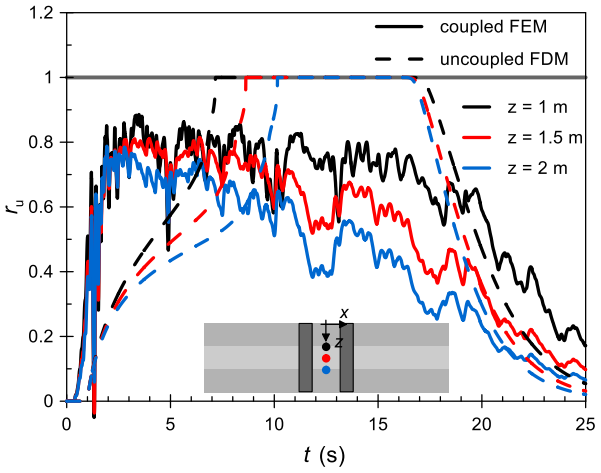

Fig. 5. Time histories of the excess pore water pressure ratio in the middle of the soil domain and different depths, obtained with the coupled FE analysis and with the simplified, uncoupled FD method.

Fig. 6 compares the time histories of the excess pore water pressure ratio, r_u, computed at two points outside the area occupied by drains, at distances equal to 4.25 m and 6.75 m from the centre of the problem domain, at middle depth within the liquefiable layer ($z = 1.50$ m). The difference between the time histories of r_u at these two points is negligible, indicating a little influence of the drains at this distance, as expected.

In the coupled FE analysis, liquefaction is triggered after 3 s, and the dissipative phase is much less evident than observed between the drains (Fig. 5). In this case, the results of the simplified method are in a much better agreement with the FE analysis, probably due to the low influence of the drains. Indeed, an overestimation of the number of equivalent cycles N_{eq} results in a predominant generative term over the dissipative one in the Eq.(1), with a negligible pore water pressures dissipation during the equivalent cyclic load (as shown also in Fig (5) for the uncoupled FDM results). Due to the presence of the clay cap, this quasi-undrained condition is achieved also in the zones far from the drain (with respect to its diameter) in the coupled FE model.

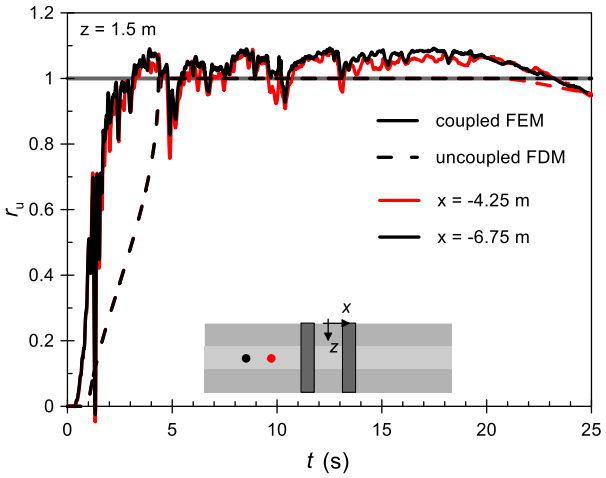

Fig. 6. Time histories of the excess pore water pressure ratio, outside the area occupied by the drains and in the middle of the liquefiable layer, at different distances from the centre of soil domain, obtained with the FE numerical analysis (coupled FEM) and with the simplified method (uncoupled FDM).

4 CONCLUSIONS

The main objective of this work was addressing the reliability of the simplified method proposed by Seed and Booker (1977) to design gravel drains for mitigating liquefaction. To this end, the simplified method was implemented in a homemade *Matlab* routine via the Finite Difference Method, and a fully coupled 3D dynamic FE analysis was carried out with the software *Plaxis* for comparison. The differences observed between the two analyses confirmed that some of the assumptions underlying the simplified method affect its predictive capability. In particular, the simplified method should be improved by considering more realistic hypotheses for the representation of the time histories shear stress with an equivalent cyclic load.

ACKNOWLEDGEMENTS

Numerical analyses were carried out thanks to the support by Bentley and Dr. Sandro Brasile. This support is gratefully acknowledged.

REFERENCES

1) Benz, T., Vermeer, T. A. and Schwab, R. (2009): A small-strain overlay model, *International Journal for Numerical and Analytical Methods in Geomechanics*, 33(1), 25-44.
2) Boccieri, G., Gaudio, D. and Conti, R. (2022): A simplified method for the estimation of earthquake-induced pore pressure, *Geotechnical Engineering for the Preservation of Monuments and Historic Sites III*. CRC Press, 812-822. DOI: 10.1201/9781003308867-62.
3) Boccieri, G., Gaudio, D. and Conti, R. (2023): A 1D Simplified Approach for Liquefaction Potential Evaluation of Soil Deposits, In *National Conference of the Researchers of Geotechnical Engineering*, Cham: Springer Nature Switzerland, 410-418, DOI: 10.1007/978-3-031-34761-0_50
4) Bentley Systems (2021), Plaxis 3D – Reference Manual, Delft University of Technology, Delft, The Netherlands.
5) Bouckovalas, G. D., Papadimitriou, A. G., Niarchos, D. G. and Tsiapas, Y. Z. (2011): Sand fabric evolution effects on drain design for liquefaction mitigation, *Soil Dynamics and Earthquake Engineering*, 31(10), 1426-1439.
6) Dafalias, Y. F. and Manzari, M. T. (2004): Simple plasticity sand model accounting for fabric change effects, *Journal of Engineering Mechanics*, 130(6), 622-634.
7) Elgamal, A., Lu, J. and Forcellini, D. (2009): Mitigation of liquefaction-induced lateral deformation in a sloping stratum: Three-dimensional numerical simulation, *Journal of Geotechnical and Geoenvironmental Engineering*, 135(11), 1672-1682.
8) Gaudio, D. and Rampello, S. (2019): The influence of soil plasticity on the seismic performance of bridge piers on caisson foundations, *Soil Dynamics and Earthquake Engineering*, 118, 120-133.
9) Hancock, J. and Bommer, J. J. (2005): The effective number of cycles of earthquake ground motion, *Earthquake Engineering and Structural Dynamics*, 34(6), 637-664.
10) Kramer, S. L. (1996): Geotechnical earthquake engineering. Pearson Education India.
11) Mathworks Inc. (2021): MATLAB. 2021 version 9.10.0 (R2021a), Natick, Massachusetts: The MathWorks Inc.
12) Mazzola, R. and Lombardi, G. (2021): Studio teorico e numerico dei fenomeni di liquefazione in terreni sabbiosi, MS Thesis, University of Rome Tor Vergata. *(in Italian)*
13) Miner, M.A. (1945): Cumulative damage in fatigue, Trans. ASME 67, A159-A164.
14) Onoue, A. (1988): Diagrams considering well resistance for designing spacing ratio of gravel drains, *Soils and Foundations*, 28(3), 160-168.
15) Seed, H. B. and Idriss, I. M. (1971): Simplified procedure for evaluating soil liquefaction potential, *Journal of the Soil Mechanics and Foundations division*, 97(9), 1249-1273.
16) Seed, H. B., Martin, P.P. and Lysmer, J. (1975): The generation and dissipation of pore water pressures during soil liquefaction, College of Engineering, University of California.
17) Seed, H. B. and Booker, J. R. (1977): Stabilization of potentially liquefiable sand deposits using gravel drains, *Journal of the Geotechnical Engineering Division*, 103(7), 757-768.
18) Terzaghi, K. (1923): Die Berechnung der Durchassigkeitsziffer des Tones aus dem Verlauf der hydrodynamischen Spannungs. erscheinungen. Sitzungsber. Akad. Wiss. Math. Naturwiss. Kl. Abt. 2A 132, 105-124.
19) Trifunac, M.D. and Brady A.G. (1975): A study on the duration of strong earthquake ground motion, *Bulletin of the Seismological Society of America*, 65(3), 581-626.
20) Zienkiewicz, O. C., Chang, C. T., & Bettess, P. (1980). Drained, undrained, consolidating and dynamic behaviour assumptions in soils. *Geotechnique*, 30(4), 385-395.